

Impact of Cyclone Mora in the Bay of Bengal on 2 June 2017 Mei-yu Heavy Rainfall Event in Taiwan

Hsin-Chien Liang, Sho Arakane, Huang-Hsiung Hsu, Chia-Ying Tu, and Zheng-Yu Yan

Research Center for Environmental Changes, Academia Sinica

Abstract

Torrential rainfall occurred in Taiwan on 2 June 2017. Two people were killed and three people went missing because of the flooding and landslide induced by the heavy rainfall. The Central Weather Bureau (CWB) in Taiwan reported that the Mei-yu front with a southwesterly wind induced the heavy rainfall. Meanwhile, prior to the heavy rainfall in northern Taiwan, Cyclone Mora was formed on 28 May, and dissipated on 31 May 2017 in the Bay of Bengal. This study reports that Cyclone Mora had a downstream influence in enhancing the rainfall in Taiwan. In this study, we examine the relationship through circulation analysis and use Geophysical Fluid Dynamic Laboratory (GFDL) Finite-volume dynamical core (FV3) with National Centers for Environmental Prediction (NCEP) Global Forecast System (GFS) physics (FV3GFS) to hindcast the rainfall event with realistic initial condition (NCEP analysis) and an initial condition with Cyclone Mora removed. Potential vorticity inversion is applied to remove Cyclone Mora in the NCEP analysis.

Keyword: Mei-yu, Finite-volume, FV3GFS

1. Introduction

It is well known that Taiwan is one of the region that has a large amount of precipitation: the rainfall in Taiwan is caused by its topography, an Asian monsoonal flow, a front, or a tropical cyclone (TC). Moreover, a remote effect of TC sometimes leads a heavy rainfall. One of such effect is called as the predecessor rain event (PRE). The mechanism of PRE is as follows: the low-level moisture-rich air in tropics is transported by TC's outer (synoptic-scale) circulation to the north. Then, the moisture-rich air is lifted in a frontal zone, which is situated to the north of the TC with 410–1700 km away from the TC, and the heavy rainfall occurred in the frontal zone

[Galarneau et al., 2010]. Chen and Wu (2016) reported similar heavy rainfall mechanism in Taiwan: they revealed that the heavy rainfall in the northeastern Taiwan during 19–23 October 2010 was triggered by an interaction between transportation of moisture-rich air by Typhoon Megi (2010) and Taiwan's steep topography.

Recently, a torrential rainfall occurred and the rainfall induced flooding and landslide in northern Taiwan on 2 June 2017. Two people were killed and three people went missing by this hazard. The Central Weather Bureau (CWB) in Taiwan reported that the Mei-yu front with a southwesterly wind induced the heavy rainfall. Meanwhile, prior to the heavy rainfall

in northern Taiwan, TC Mora was formed on 28 May, and dissipated on 31 May 2017 in the Bay of Bengal (BoB). In this study, we examine the relationship between TC Mora and the heavy rainfall over northern Taiwan. Our analyses are mainly done by using a set of numerical experiment that includes a simulation in which TC Mora is removed.

2. Data and Methods

a. Numerical simulation

The Geophysical Fluid Dynamic Laboratory (GFDL) Finite-volume dynamical core (FV3; Lin and Rood, 1997; Lin, 1997,2004) with National Centers for Environmental Prediction (NCEP) Global Forecast System (GFS) physics (so-called FV3GFS; Hazelton et al., 2018), which is a global model, is used in this study to reveal the effect of TC Mora on the heavy rainfall over northern Taiwan. The radiation scheme is the Rapid Radiative Transfer Model for GCMs (RRTMG; Iacono et al., 2008). The cumulus parameterization is the simplified Arakawa–Schubert scheme (Arakawa and Schubert, 1974; Han and Pan, 2011). For microphysics scheme, we employed the 6-class single-moment microphysics scheme developed by GFDL (Lin et al., 1983; Chen and Lin, 2013). The simulation is executed with approximately 13-km horizontal resolution, and the FV3GFS has 64 vertical levels with a model top is approximately 0.3 hPa. Using the NCEP GFS output, the experiment is initialized at 00 UTC 27 May 2017, and integrated for 10 days. The period of the experiment includes the occurrence and dissipation of TC Mora over the Bay of Bengal and the excitation of strong rainfall event observed in northern Taiwan. Hereinafter, we refer to

this experiment as the control experiment.

b. Sensitivity experiment

To investigate the influence of TC Mora on the torrential rainfall in northern Taiwan, we execute an additional sensitivity experiment. Using potential vorticity inversion technique employed in Hirota et al. (2016), TC Mora is removed from the initial input data used in the control experiment. After the removal of TC Mora, all physical variables (i.e., horizontal and vertical winds, temperature, pressure, and humidity) are modified in the initial data. To qualify the model uncertainty, the sensitivity experiment is executed with 11 ensemble members embedding small perturbations near TC Mora in these initial conditions. However, just one member's result will be used in the following analysis because the results of the ensemble members were quantitatively similar.

c. Data for verification of the control experiment

We use the observational data provided by CWB, and JRA-55 (Kobayashi et al., 2015; Harada et al., 2016) provided by the Japan Meteorological Agency to verify the validity of the control experiment result. The JRA-55 is a 6-hourly 1.25° latitude/longitude gridded data set.

d. Backward trajectory analysis

To establish the origin of the air parcels constituting the heavy rainfall system, the backward trajectory analyses are executed for 3-hourly outputs of the control and the sensitivity experiments and for the 6-hourly JRA-55. Fifteen-minute intervals of linear temporal interpolation are considered for the trajectory calculations.

e. Frontogenetical function budget analysis

In order to reveal the development of a frontal system near Taiwan, the budget analysis for the frontogenetical function developed by Ogura and Portis (1982) is executed. The budget equation is expressed as

$$F_G = F_{\text{div}} + F_{\text{def}} + F_{\text{tilt}} + F_{\text{diab}}$$

where F_G is the frontogenetical function, F_{div} is the divergence term, F_{def} is the deformation term, F_{tilt} is the tilting term, and F_{diab} is the diabatic term. Each term is expressed in the pressure coordinates as

$$F_G = \frac{d}{dt} |\nabla_h \theta_e|,$$

$$F_{\text{div}} = -\frac{1}{2} |\nabla_h \theta_e| \delta,$$

$$F_{\text{def}} = -\frac{1}{|\nabla_h \theta_e|} \left[\frac{1}{2} \left\{ \left(\frac{\partial \theta_e}{\partial x} \right)^2 - \left(\frac{\partial \theta_e}{\partial y} \right)^2 \right\} D_1 + \frac{\partial \theta_e}{\partial x} \frac{\partial \theta_e}{\partial y} D_2 \right],$$

$$F_{\text{tilt}} = -\frac{1}{|\nabla_h \theta_e|} \frac{\partial \theta_e}{\partial p} \nabla_h \theta_e \cdot \nabla_h \omega,$$

$$F_{\text{diab}} = \frac{1}{|\nabla_h \theta_e|} \nabla_h \theta_e \cdot \nabla_h \left(\frac{d\theta_e}{dt} \right),$$

where ∇_h is the horizontal differential operator, $d/dt = \mathbf{u}_h \cdot \nabla_h + \omega \partial/\partial p$ is the total derivative, \mathbf{u}_h is the horizontal wind vector, ω is the pressure velocity, and θ_e represents the equivalent potential temperature. $\delta \equiv \partial u/\partial x + \partial v/\partial y$ is the divergence, $D_1 \equiv \partial u/\partial x - \partial v/\partial y$ is the stretching deformation, and $D_2 \equiv \partial v/\partial x + \partial u/\partial y$ is the shearing deformation. In the following budget analysis, we will focus on its dynamical effects (i.e., F_{div} , F_{def} , and F_{tilt}) because the diabatic heating ($d\theta_e/dt$) expressed in F_{diab} is hard to calculate accurately.

3. Results

The observed 24-h accumulated rainfall and the results in the numerical experiments are shown in Figure 1. Although the amount of rainfall in the control experiment is smaller than the observed one, a tripole

rainfall pattern over Taiwan, which located at about (23°N, 120.8°E), (24°N, 121°E), and (25°N, 121.5°E), are well reproduced (Figure 1a,b). On the other hand, the rainfall amount becomes smaller in the sensitivity experiment; especially in northern area, the rainfall amount is quite reduced because the rainfall region shifted to the north compared with the result of the control experiment (Figure 1b,c).

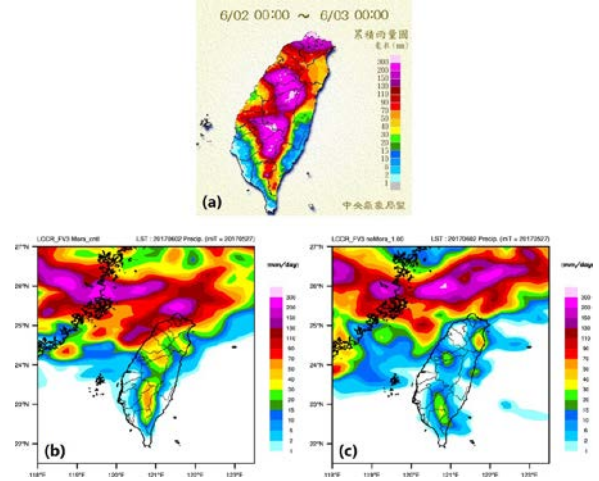


Figure 1. The 1-day accumulated rainfall (mm day⁻¹) from 00 LST (GMT+8) 2 June 2017. (a) Observed rainfall provided by Central Weather Bureau, (b) the result of the control experiment, and (c) the result of the sensitivity experiment.

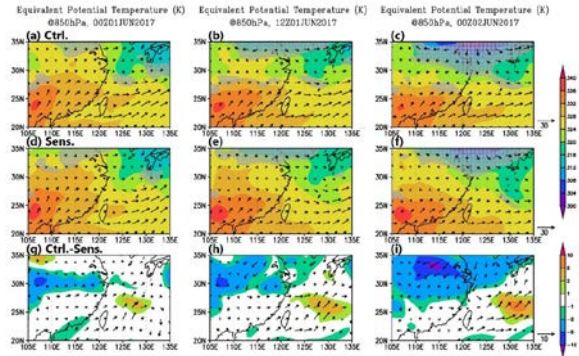


Figure 2. The daily-averaged equivalent potential temperature (θ_e ; color, K) and horizontal wind (vector, m s⁻¹) at 850 hPa at (a) 00 UTC 1, (b) 12 UTC 1, and (c) 00 UTC 2 June 2017 in the control experiment. The middle (bottom) panel is the same as the top panel but for the sensitivity experiment (the difference between the control and sensitivity experiments). The grey-colored hatched region indicates where the magnitude of θ_e gradient is larger than 5 K (100 km)⁻¹.

To represent that the northwardly shifted rainfall region is caused by a change of the frontal system near

Taiwan in the sensitivity experiment, low-level equivalent potential temperature (θ_e) and magnitude of θ_e gradient are shown in Figure 2. The frontal zone to the north of Taiwan (at about 28°N) is observed in the control experiment (Figure 2a,b,c). In the sensitivity experiment, the frontal zone becomes weaker (Figure 2d,e,f) because the cold air mass located to the north of the frontal zone shifts to the north and thus the magnitude of θ_e gradient becomes weaker (Figure 2g,h,i). Note that the main difference of θ_e field between these experiments is caused by the cold air mass but a warm air mass located at (23°N, 107°E) remains unchanged (Figure 2g,h,i).

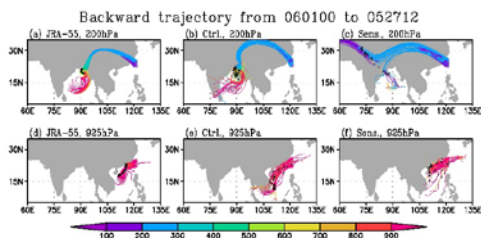


Figure 3. Forty 108-h backward air parcel trajectories beginning at 200 hPa at 00 UTC 1 June 2017 by (a) JRA-55, (b) the control experiment result, and (c) the sensitivity experiment result. The color in the trajectories indicates a level of the air parcel, and the black dots are the positions of the air parcels at 00 UTC 30 May 2017. The initial positions of the air parcels are located over an entire Taiwan. (Bottom panel) As in the top panel but beginning at 925 hPa.

Moreover, to establish the origin of the air parcels over Taiwan, the results of the backward trajectory analyses are shown in Figure 3. The results show that all the air parcels at 200 hPa came from BoB in the control experiment (Figure 3b); this is consistent with the analysis by JRA-55 (Figure 3a). In contrast, most of the air parcels came from Europe in the sensitivity experiment (Figure 3c). This suggests that an upper-level circulation changes in the sensitivity experiment. On the other hand, the analysis beginning at 925 hPa shows that a large number of the air parcels in the control experiment came from more southern region compared with the sensitivity experiment (Figure 3e,f). This suggests that a low-level circulation induced by

TC Mora transports warm moist air to Taiwan from more southern region. The above-mentioned results suggest the possibility that TC Mora influences on the heavy rainfall in northern Taiwan.

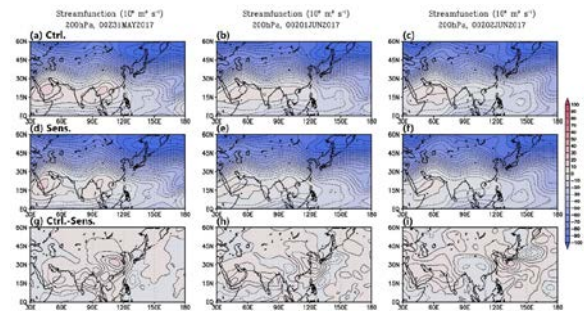


Figure 4. The daily-averaged streamfunction (color and contour, contour interval is $5 \times 10^6 \text{ m}^2 \text{ s}^{-1}$) at 200 hPa on (a) 31 May, (b) 1 June, and (c) 2 June 2017 in the control experiment. The middle (bottom) panel is the same as the top panel but for the sensitivity experiment

To confirm the possibility that TC Mora influences on the heavy rainfall, we execute further analyses on it. The streamfunction difference between these experiments clearly shows that the difference becomes larger and spreads widely with time (Figure 4). This means that the existence of TC Mora influences on the large-scale circulation and then the TC Mora's effect is propagated far away accompanied by large-scale atmospheric wave. Thus, as suggested in Figure 3, the change of the upper-level circulation was confirmed. Similar with the upper-level wind field, wind field at low level also changes. Figure 5 shows the wind field at 900 hPa. In common with both experiments, there exists southwesterly from the South China Sea toward Taiwan and the development of northerly wind over the East China Sea and the Yellow Sea is observed. As shown in the difference between these results, both the southwesterly and northerly wind are strengthened when TC Mora exists. The enhancement of the southwesterly when TC Mora exists is consistent with the suggestion shown in Figure 3f. Moreover, there are no contradictions between the enhancement of the northerly wind by TC Mora's effect and the change of the expansion the cold air mass shown in Figure 2c,f.

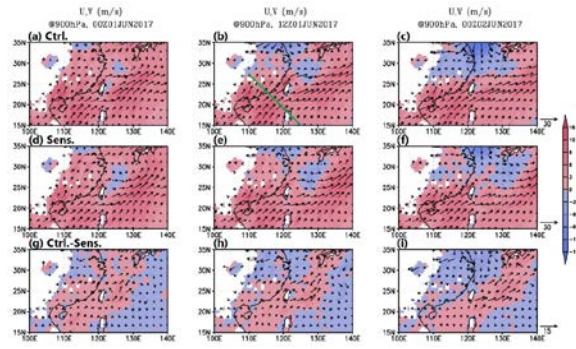


Figure 5. The daily-averaged horizontal wind (vector, m s⁻¹) and meridional wind (color, m s⁻¹) at 900 hPa at (a) 00 UTC 1, (b) 12 UTC 1, and (c) 00 UTC 2 June 2017 in the control experiment. The middle (bottom) panel is the same as the top panel but for the sensitivity experiment

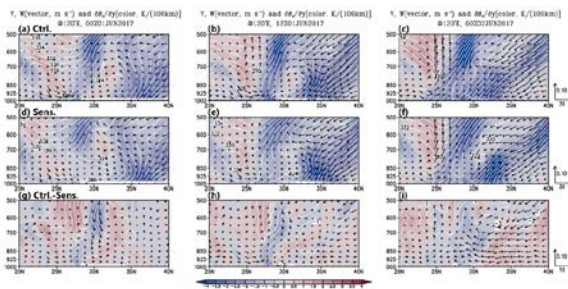


Figure 6. Vertical cross-section of daily-averaged wind field parallel to the section (vector, m s⁻¹) and latitudinal gradient of θ_e [color, K (100 km)⁻¹] along 120°E at (a) 00 UTC 1, (b) 12 UTC 1, and (c) 00 UTC 2 June 2017 in the control experiment. The middle (bottom) panel is the same as the top panel but for the sensitivity experiment (the difference between the control and sensitivity experiments). Note that the plotted data are horizontally averaged over 2°×2° area.

Finally, we investigate the difference of the frontal development between both the numerical experiments and show the influence of TC Mora on the frontal system. The frontal structures along 120°E are shown in Figure 6. The region where θ_e gradient is steep is observed from 25 to 40°N at 00 UTC 1 June 2017 in the control experiment (Figure 6a); the front moves southwardly and becomes stronger with time (Figure 6b,c). Compared with the control experiment, a frontal system is weaker in the sensitivity experiment (Figure 6d,e,f), especially as shown in Figure 6c and Figure 6f, it is clear that the southward movement of the front and thus the frontal concentration becomes weaker when TC Mora is removed. The difference of the frontal movement and thus the concentration is caused

by the change of wind field, that is, southward wind to the north of the frontal system shown in Figure 6g,h,i.

Note that the enhancement of the southward wind by TC Mora is consistent with the result shown in Figure 5. The stronger southward wind in the control experiment propagates the front effectively, and it is suggested that the front is developed by divergence and deformation processes. To confirm how the front is developed, the frontogenetical function budget analysis is carried out.

4. Discussion and Summary

The mechanism of torrential rainfall occurred in northern Taiwan on 2 June 2017 was investigated to clarify the relationship between the rainfall and Tropical Cyclone Mora developed over the Bay of Bengal. Because the numerical experiment reproduced the heavy rainfall over northern Taiwan well, the mechanism was investigated using a set of numerical experiments: one was the control experiment and the other was the sensitivity experiment in which TC Mora was removed. The analysis provided us the mechanism of the rainfall as following steps:

- (1) TC Mora changed dynamical field extensively;
- (2) The changed dynamical field made stronger southwesterly over the South China Sea toward Taiwan and stronger southward wind to the north of Taiwan;
- (3) The stronger southwesterly transported low-level moisture toward Taiwan effectively and thus enhanced low-level moisture convergence near Taiwan;
- (4) The stronger southward wind changed a location and a movement of cold air mass located to the north of Taiwan;
- (5) The strengthened southward wind and movement of the cold air mass created a strong frontal

system to the north of Taiwan through the deformation and divergence effect on the frontal evolution; and

As stated above, it is certain that TC Mora contribute to the torrential rainfall. This rainfall mechanism may be one of the TCs' remote effects. In fact, the low-level moisture-rich air transported by TC's outer circulation to the north and the moisture-rich air lifting in the frontal zone, which were the same mechanism of PRE, were found in the analysis. However, some different aspects between PRE and this phenomenon were observed. Although, as stated in Section 1, distances between TC and frontal zone in PRE were 410–1700 km statistically, the distance between TC Mora and the frontal zone to the north of Taiwan in this event was approximately 3500 km. Moreover, a remarkable difference is that the existence of TC Mora contributed to the formation and the evolution of the frontal zone; a weakened front forms to the north of the observed front position if TC Mora does not exist. From these points of view, we can claim that this heavy rainfall event is different from PRE. Although there are many studies about the heavy rainfall caused by PRE, a rainfall event caused by other remote mechanism of TC is rarely reported. This study will be one of the studies which shed light on the other remote mechanisms of TC.

6. Reference

- Arakawa, A., and W. H. Schubert (1974), Interaction of a cumulus cloud ensemble with the large-scale environment, Part I. *J. Atmos. Sci.*, **31**, 674–701, doi:10.1175/1520-0469(1974)031<0674:IOACCE>2.0.CO;2.
- Chen, J.-H., and S.-J. Lin (2013), Seasonal predictions of tropical cyclones using a 25-km-resolution general circulation model. *J. Climate*, **26**, 380–398, doi:10.1175/JCLI-D-12-00061.1.
- Chen, T.-C., and C.-C. Wu (2016), The remote effect of Typhoon Megi (2010) on the heavy rainfall over northeastern Taiwan, *Mon. Weather Rev.*, **144**, 3109–3131, doi: 10.1175/MWR-D-15-0269.1.
- Galarneau, T. J., Jr., L. F. Bosart, and R. S. Schumacher (2010), Predecessor rain events ahead of tropical cyclones, *Mon. Weather Rev.*, **138**, 3272–3297, doi:10.1175/2010MWR3243.1.
- Han, J., and H.-L. Pan (2011), Revision of convection and vertical diffusion schemes in the NCEP Global Forecast System. *Weather Forecast.*, **26**, 520–533, doi: 10.1175/WAF-D-10-05038.1.
- Harada, Y., H. Kamahori, C. Kobayashi, H. Endo, S. Kobayashi, Y. Ota, H. Onoda, K. Onogi, K. Miyaoka, and K. Takahashi (2016), The JRA-55 reanalysis: Representation of atmospheric circulation and climate variability, *J. Meteorol. Soc. Jpn.*, **94**, 269–302, doi: 10.2151/jmsj.2016-015.
- Hazelton, A. T., L. Harris, and S.-J. Lin (2018), Evaluation of tropical cyclone structure forecasts in a high-resolution version of the multiscale GFDL fvGFS model, *Weather Forecast.*, **33**, 419–442, doi: 10.1175/WAF-D-17-0140.1.
- Hirota, N., Y. N. Takayabu, M. Kato, and S. Arakane (2016), Roles of an atmospheric river and a cutoff low in the extreme precipitation event in Hiroshima on 19 August 2014. *Mon. Weather Rev.*, **144**, 1145–1160, doi:10.1175/MWR-D-15-0299.1.
- Iacono, M. J., J. S. Delamere, E. J. Mlawer, M. W. Shephard, S. A. Clough, and W. D. Collins (2008), Radiative forcing by long-lived greenhouse gases: Calculations with the AER radiative transfer models. *J. Geophys. Res.*, **113**, D13103, doi:10.1029/2008JD009944.
- Kobayashi, S., and Coauthors (2015), The JRA-55 reanalysis: General specifications and basic characteristics, *J. Meteorol. Soc. Jpn.*, **93**, 5–48, doi:10.2151/jmsj.2015-001.
- Lin, S.-J. (1997), A finite-volume integration method for computing pressure gradient force in general vertical coordinates. *Q. J. R. Meteorol. Soc.*, **123**, 1749–1762, doi: 10.1002/qj.49712354214.
- (2004), A “vertically Lagrangian” finite-volume dynamical core for global models. *Mon. Weather Rev.*, **132**, 2293–2307, doi:10.1175/1520-0493(2004)132<2293:AVLFDC>2.0.CO;2.
- , and R. B. Rood (1997), An explicit flux-form semi-Lagrangian shallow-water model on the sphere. *Q. J. R. Meteorol. Soc.*, **123**, 2477–2498, doi:10.1002/qj.49712354416.
- Lin, Y.-L., R. D. Farley, and H. D. Orville (1983), Bulk parameterization of the snow field in a cloud model. *J. Clim. Appl. Meteorol.*, **22**, 1065–1092, doi:10.1175/1520-0450(1983)022<1065:BPOTSF>2.0.CO;2.
- Ogura, Y., and D. Portis, 1982, Structure of the cold front observed in SESAME-AVE III and its comparison with the Hoskins–Bretherton frontogenesis model. *J. Atmos. Sci.*, **39**, 2773–2792, doi:10.1175/1520-0469(1982)039<2773:SOTCFO>2.0.CO;2.